Research Square

Preprints are preliminary reports that have not undergone peer review.
They should not be considered conclusive, used to inform clinical practice,
or referenced by the media as validated information.

Remarkable Capability of Activated Carbon Nanoparticles-Incorporated PLA Nanofibrous Structure as Hemodialysis Supplement for Uremic Toxins Removal

Pooya Javadi
Shiraz University
Fatemeh Hejazi
f.hejazi@shirazu.ac.ir

Shiraz University
Leila Malekmakan
Shiraz University of Medical Sciences

Research Article

Keywords: Uremic Toxin, Nanostructured Adsorbent, Polylactic acid, Activated Carbon Nanoparticles, Hippuric Acid

Posted Date: August 20th, 2026

DOI: https://doi.org/10.21203/rs.3.rs-10582084/v1

License: This work is licensed under a Creative Commons Attribution 4.0 International License.
Read Full License

Additional Declarations: No competing interests reported.

Abstract

Chronic kidney disease (CKD) is an expanding condition affecting a large population worldwide, with a significant proportion of these patients progressing to kidney failure and requiring considerations such as hemodialysis (HD). HD presents several challenges, such as an inflexible treatment regimen and limited toxin removal. Recent advancements have confirmed the use of adsorbents to increase the efficiency of the dialysis process. In the present research, adsorbents composed of polylactic acid (PLA) nanofibers containing activated carbon nanoparticles (AC NPs) were designed. Formation of uniform PLA nanofibers and presence of AC NPs on the surface of PLA nanofibers were evidenced. According to roughness evaluation, surface roughness of the prepared adsorbent was beyond the threshold of hemolysis, platelet and protein adhesion, and activation of the coagulation cascade. In addition, despite the enhanced surface hydrophilicity of the nanofibrous structure containing AC NPs, according to partial thromboplastin time test, the prepared adsorbent did not accelerate the clot formation. Evaluation of the fabricated nanostructural adsorbents for uremic toxin removal revealed high equilibrium adsorption and significant removal percentage. PLA nanofibrous mat containing 10 wt% AC NPs (possessing total weight of 3.5 mg), removed 31% of hippuric acid content and 90.5% of urea from the exposed solution and provided equilibrium adsorption capacity of 0.2 and 2.41 for the mentioned toxins, respectively. Adsorbents composition together with their unique microstructure providing high surface area and dual size porosity would account for the observed efficiency in uremic toxin removal.

Introduction

Chronic kidney disease (CKD) as a major public health challenge, is marked by significant increasing incidence and prevalence worldwide, especially in developing nations. This condition culminates in end-stage renal disease (ESRD), which is associated with premature mortality, impaired quality of life, and an inevitable burden on healthcare systems [1]. As reported in a 2021 international study, an estimated 18.9 million cases of CKD were documented globally in 2019 [2]. The occurrence of chronic kidney disease is projected to rise in the near future. This projected rise is ascribed to several factors, including an aging populace, the growing incidence of diabetes, hypertension, and other contributors [3]. UTs are substances normally excreted by the kidneys that accumulate in the body upon renal failure. These toxins contribute to various pathological consequences, including cardiovascular injury, the development of multiple diseases, and reduced life expectancy associated with acute kidney disease. UTs are classified into several categories: small water-soluble compounds (e.g., urea), medium molecular weight compounds and protein-bound uremic toxins (PBUTs), such as hippuric acid (HA) [4, 5].

Due to elimination of these pathological issues, considerable research has been undertaken in recent years aimed at treating chronic kidney disease (CKD), extending patient survival, or enhancing therapeutic protocols. The efficacy of novel materials and approaches for influencing this disease is under ongoing evaluation. Hemodialysis (HD) remains a common modality for clearing uremic toxins from the bloodstream, despite its limitations. Conventional hemodialysis predominantly targets the removal of low- and medium-molecular-weight water-soluble compounds [6]. The removal of protein-

bound uremic toxins from the circulation during hemodialysis occurs at very low percentages, a consequence of their low plasma concentration. This finding reflects the limited efficacy of conventional hemodialysis in eliminating protein-bound uremic toxins bound to human serum albumin (HSA) [7]. Moreover, in the stage of renal failure, urea that is not metabolizable by the human body can be reduced to normal concentrations with a high-flux hemodialyzer following 4 hours of operation [8], nevertheless, the current length of hemodialysis sessions raises the mortality rate among patients, particularly the elderly, due to the need to clear substantial quantities of urea [9].

Adsorption-based separation techniques are currently under investigation for blood purification. The use of adsorbents placed within a column to facilitate a coordinated interaction between a dialysate or blood, as well as the positioning of adsorbents on the layer surface, has been evaluated for the removal of uremic toxins with the aim of developing wearable and portable devices. Over recent years, a range of adsorbent materials have been employed, comprising inorganic-based sorbents (e.g., activated carbon, silica, zeolite, MXene, graphene/graphene oxide, and fullerene) and organic-based sorbents (e.g., chitosan, molecularly imprinted polymers, starch, celluloses, and metal-organic frameworks) [10–12]. Among the available materials, activated carbon has consistently been one of the most thoroughly studied over the course of artificial kidney research, and it has been identified as a promising adsorbent for uremic toxins. The removal of uremic toxins via adsorption necessitates nanoporous biomaterials, wherein activated carbon holds particular significance. These nanoporous biomaterials are additionally utilized in hemoperfusion for the extraction of uremic toxins. To achieve further downsizing of artificial kidney systems and to improve the capacity for uremic toxin adsorption, high-performance nanoporous biomaterials are required materials that offer not only greater surface area and tunable pore sizes but also a deliberately designed architecture or structure together with surface functional groups [6, 13]. Per Yatzidis, charcoal was the initial adsorbent employed for the removal of uremic toxins in artificial kidneys. Following its first introduction in 1964, adsorbent-based hemoperfusion has been aided by activated carbon. [14]. Beyond its application in blood contamination, the principle of hemoperfusion is likewise employed in artificial liver systems [15–17]. Among nanoporous biomaterials, activated carbon is the most prevalent and widely recognized, and it may be regarded as an appropriate adsorbent for uremic toxins owing to its high surface-area-to-volume ratio, strong affinity for dissolved organic and inorganic pollutants, and its inherent amphoteric characteristics [18–20].

Sandman and colleagues evaluated the in vitro adsorption efficiency of indoxyl sulfate and p-cresol sulfate using a prototype monolithic nanoporous activated carbon, reporting 85% removal of indoxyl sulfate and 78% removal of p-cresol sulfate following 60 minutes of perfusion. Additionally, they demonstrated that the monolithic nanoporous material achieved 83% removal of indoxyl sulfate and 75% removal of p-cresol sulfate after 30 minutes of continuous perfusion with 20 mL of samples obtained from patients undergoing high-flux hemodialysis. [21]. In 2017, Pavlenko et al. conducted a study aimed at further investigating carbon-based adsorbents through pore structure engineering to improve the removal of uremic toxins and other molecules, including cytokines. The adsorbent employed (designated CMK-3) was synthesized via the nano-hard template method and exhibits two distinct pore size regimes: micropores and mesopores. The findings demonstrated high adsorption capacity toward small toxins

(e.g., creatinine) as well as protein-bound uremic toxins, particularly indoxyl sulfate and hippuric acid. Importantly, total plasma protein levels did not decline following the 4-hour test, and the elimination of protein-bound uremic toxins appeared to correlate with protein binding. Additionally, the results indicated that small quantities of CMK-3 are capable of achieving selective and complete blood purification [22].

Mixed matrix membranes (MMMs) have been fabricated by incorporating zeolites, activated carbon, metal-organic frameworks (MOFs), and carbon nanotubes into the polymeric matrix.[10, 23]. In various industrial contexts, filters or membranes derived from non-biodegradable polymers are employed to reduce certain contaminants and clinical toxins, performing adequately in filtration applications. A broad range of membranes are produced from synthetic polymers, which require thousands of years to degrade, thereby generating multiple forms of pollution. Furthermore, their reusability is occasionally constrained. Consequently, recent years have seen the investigation of various biodegradable polymers for use as filtration media and for industrial application, depending on the manufacturing process. [24–26]. In the fabrication of air filtration media, various polymers have been employed, including polyurethane, polyacrylonitrile, polyvinylidene fluoride, polyvinyl chloride (PVC)/polyurethane, polycarbonate, silk, polyimide, polylactic acid (PLA), and polycaprolactone (PCL), with the last-mentioned exhibiting favorable biodegradability. [27, 28].

Polylactic acid (PLA), also referred to as polylactide, represents one of the most commonly employed biodegradable and renewable thermoplastic polyesters. It has been the most extensively researched among bio-based polyesters and exhibits considerable potential as a substitute for traditional petrochemical-derived polymers [29]. Nevertheless, little research has been performed on the fabrication and utilization of porous polylactic acid membranes. Owing to their excellent biocompatibility, polylactic acid and its copolymers, such as poly(lactic-co-glycolide), have been processed into porous membranes for tissue engineering applications via thermally induced phase separation [30–33]. The biocompatibility of bio-based polylactic acid has additionally demonstrated significant potential for broad use in sutures[34], bone fracture fixation devices, and other applications, thereby positioning this polymer as an appropriate candidate for medical applications [35].In one investigation, for instance, the synthesis and use of polymeric nanocomposites composed of polylactic acid (PLA) and modified nanoclay (cloisite 20A) functionalized with 1,4-diaminobutane dihydrochloride were examined across varying reaction durations. The polylactic acid incorporating clay nanoparticles achieved 77% removal of urea. [36]. In a separate study, the mixed matrix membranes (MMMs) demonstrated outstanding in vitro biocompatibility and a high-water flux reaching 260 L m^{-2} h^{-1}. Under static conditions, the MMMs achieved 75% removal of hippuric acid (HA) and 78% removal of indoxyl sulfate (IS) over 4 hours, whereas the PLA membrane removed 12% of HA and 13% of IS [37]. In 2021, Siyu Xiong modified a standard electrospinning apparatus by integrating it with a commercial three-dimensional printing system to produce a polycaprolactone-based composite fibrous membrane in a programmable configuration for investigations into indoxyl sulfate absorption. A single polycaprolactone/chitosan (PCL/CS) composite fibrous adsorbent material attained 28% clearance of free-form indoxyl sulfate molecules at initial concentrations of both 40 mg/L and 5 mg/L during a single pass over a 1-hour period [38].

The aim of the present study is to use nanostructured adsorbents and design suitable nanocomposites to improve and supplement hemodialysis. For this purpose, porous active carbon nanoparticles (ACNPs) were incorporated into PLA nanofibers with suitable characteristics in terms of biocompatibility and hemocompatibility. In the following, the chemical, physical and microstructural properties of the prepared nanocomposites will be evaluated and the efficiency of the prepared nanostructural adsorbent in contact with uremic toxins will be investigated.

Materials and Methods

Poly (lactic acid) (PLA, Mn = 60 kilodalton, Sigma-Aldrich, United States), Activated Carbon Nanoparticle (diameter of 20–40 nanometer, Iranian Nanomaterials Pioneers Company, Iran), Dimethylformamide (Pure, Merck, Unite States), Chloroform (Pure, Merck, United States), Distilled water (pH = 7) were used to prepare the adsorbents. PBS from Quebec Canada Medicago, Tyrode Buffer and urea from Merck and Hippuric acid from Sigma-Aldrich were purchased in order to proceed the adsorption test.

Preparation of Adsorbents Based on PLA

In order to prepare the polylactic acid nanofibrous structure, electrospinning method was used [39]. Electrospinning is one of the versatile techniques to produce nanofibrous nanofibrous structures with innovative designs and high surface area [40–42]. This technique provides the possibility for the fabrication of fibrous nanocomposites by incorporating vast majority of nanoparticles in the spinning nanofibers [43–47].

In the present work, 14% w/v solution of polylactic acid was prepared in the solvent system chloroform:dimethylformamide with a volume ratio of 9:1 and the solution was homogenized for 3 hours at 25°C on a magnetic stirrer at 600 rpm. Subsequently, the resulting solution was poured into a 5 ml syringe and placed in the injection pump of the electrospinning device. Electrospinning of the solution was performed at voltage difference of 10 KV, the needle tip to collector distance of 15 cm, and injection rate of 0.4 ml/h.In order to prepare polylactic acid nanofibrous structure containing activated carbon nanoparticles, polymer solution was prepared according to the pure polylactic acid method. After the solution was homogenized, activated carbon nanoparticles at two amounts of 5 and 10% by weight relative to the PLA content were gradually added to the polymer solution and the system was placed on magnetic stirrer for another 20 minutes. In order to properly distribute the activated carbon particles in the solution, solution container was placed in an ultrasonic bath for 20 minutes at a frequency of 37 kHz and 100% power.

Characterization

Optical Microscopy

Optical microscope (OLYMPUS BX61, Japan) was used to evaluate the morphology of the prepared active carbon NPs incorporated-nanofibrous adsorbents.

Scanning Electron Microscopy

In the present study, scanning electron microscope (VEGA3-TESCAN, Czech Republic) was used to examine the microstructure of the fabricated adsorbents. Gold sputter coating device (R-ES150, Quorum Technologies) was used to prepare the sample. The SEM images were then analyzed using ImageJ software (Developed by National Institutes of Health and the Laboratory for Optical and Computational Instrumentation, University of Wisconsin), and the average diameter and diameter distribution of the nanofibers were determined (using Origin software, Microsoft Windows).

Atomic Force Microscopy

In this study, an atomic force microscope (manufactured by Arapajouhesh Company - Iran) was used to examine the surface of the prepared nanostructual adsorbents. Surface roughness data obtained by this technique can be correlated with their blood compatibility.

Surface Hydrophilicity

Hydrophilicity of the components utilized in the blood purification system guarantees the proper contact of the blood with the adsorbents and determines the ability to bind uremic toxins. In light of that, the prepared adsorbents must have the required hydrophilic property. Water contact angle has a direct relationship with surface hydrophobic/hydrophilic characteristic [48]. In the present study, to investigate the hydrophilicity of the prepared adsorbent nanostructure and to evaluate the effect of AC NPs in improving the hydrophilicity, water contact angle test was performed. For this purpose, a drop of deionized water was placed on the surface of the nanofiber samples using a syringe. Imaging was performed using a digital microscope and the contact angles were measured at the first moment and also after 1 minute using the ImageJ program. This test was performed three times for each sample and the average contact angle was reported.

Clot Formation Duration

In order to investigate the clot formation duration of blood in contact with the prepared adsorbent, partial thromboplastin time test was done. For this aim, coagulometer (Sysmex CS2400i, Germany) and Thermo Fisher kit (Unite States) were used. In this test, platelet-poor plasma was obtained by centrifugation of fresh human blood at 3500 rpm for 10 minutes. Fabricated sorbent was cut into 2×2 cm^2 pieces and each piece was exposed to 2 mL of the prepared plasma, and placed in a shaker incubator at 37°C. After 1 hour, the sorbent was removed and 300 microliters of plasma were referred to the coagulometer for reading.

Adsorption of PBUTs on Fabricated Nanocomposites

In order to investigate the efficiency of the fabricated adsorbents in uremic toxins removal, the structures were exposed to hippuric acid and urea. In order to prepare standard solutions of these toxins, 0.5 mg/ml hippuric acid solution in Tyrode and 2 mg/ml urea solution in phosphate buffer were prepared [37]. Subsequently, pieces with dimensions of 3 $\times$ 3.5 cm^2 were prepared from the fabricated adsorbents and placed around the inner wall of the microtube. Then, 2 ml of hippuric acid/ urea solution was poured into the tube and the system was placed in a shaker incubator at 37°C for 4 hours (average hemodialysis time).

In order to examine the concentration of toxins in the solution and determine the amount of absorption, UV-Vis Spectrophotometry (Unico uv2150, China) was used in the range of 190 to 400 nm. Solutions with serial concentrations of toxins were prepared and used to obtain the calibration curves. Uremic toxins removal percentage (R%) and equilibrium adsorption capacity (q_e)of uremic toxins by fabricated sorbents were calculated by the following equations:

$$R\ (\%) = \frac{(C_0 - C_e)}{C_0} \times 100$$

$$q_e = \frac{(C_0 - C_e)V}{m}$$

where C_0 and C_e (mg. L^{-1}) are the initial and equilibrium concentrations of HA and Urea, respectively, V (L) is the volume of the solution, and m (mg) is the adsorbent weight. In order to prevent device errors due to high concentrations of uremic toxins, the solutions were diluted and the final volume in the calculation of q_e was considered to be 4ml.

Results and Discussion

Morphology of the prepared adsorbents

In order to investigate the formation of nanofibers by electrospinning, a thin layer of electrospun fibers was evaluated by optical microscope. Optical microscope images of the PLA nanofibers containing 5wt% AC NPs are shown in Fig. 1. Images indicate the successful formation of nanofibers in which carbon nanoparticles are remarkably visible inside them. This observation indicates the successful incorporation of carbon nanoparticles into the nanofibers and the suitability of the manufacturing processes which prevent the aggregation of NPs.

Scanning electron microscope images of PLA nanofibers and PLA nanofibers containing 5 and 10 wt% AC NPs are shown in Fig. 2a, b, and c. According to the results, analysis of the images indicates average diameter of 663, 445, and 699 nm for the aforementioned samples, respectively. In addition, distribution of fibers diameter is presented in Fig. 2d which indicates the dual effect of AC NPs on the PLA

nanofibers diameter. Presence of AC NPs, due to the increase in the electrical conductivity of the solution, lead to greater stretching of the fibers in the electric field, which led to the formation of thinner nanofibers. On the other hand, increasing the amount of these nanoparticles from 5 to 10% increases the viscosity of the precursor solution, resulting in diameter increase.

In SEM image with higher magnification (Fig. 3), AC NPs with diameter of 40 to 70 nm on the nanofibers surface can be clearly observed. Presence of AC NPs on the surface of nanofibers can be attributed to the interaction of these conductive nanoparticles with the applied electrical field during electrospinning. Presence of these NPs on the surface of nanofibers provides the possibility of their effective contact with uremic toxins which guarantees the significant removal of these toxins.

In order to achieve more information about the surface properties of the prepared adsorbents, atomic force microscopy [49] was applied (Fig. 4). Furthermore, data on surface roughness were obtained by analyzing the AFM images (Table 1). Accordingly, average roughness of PLA nanofibrous structure and PLA nanofibrous structure containing 5 and 10 wt% AC NPs was 463, 441 and 293 nm, respectively. Decrease in surface roughness by the presence of AC NPs provides smoother surface which is crucial for blood contacting materials. As the roughness threshold for rapid hemodialysis has been reported to be between 600 and 800 nm [50, 51], surface of the adsorbents prepared in this study does not cause destruction and hemolysis of red blood cells due to the roughness much beyond this threshold, especially in PLA nanofibrous structure containing 10 wt% AC NPs. Given that the adsorption of platelets, fibrinogen, and VWF is enhanced by increasing surface roughness, surfaces with roughness of 400 nm are at the threshold of adsorption of coagulation components present in the blood [52]. Accordingly, surface of the prepared adsorbent, PLA nanofibrous structure containing 10 wt% AC NPs, would inhibit the adsorption of platelets and proteins such as fibrinogen, and as a result, prevent the activation of the coagulation cascade.

Table 1
Quantitative parameters of surface roughness of the prepared adsorbents.

Ra	**PLA**	**PLA + 5%ACNPs**	**PLA + 10%ACNPs**
	463 nm	**441 nm**	**293 nm**
Rq	547 nm	548 nm	397 nm
Rv	-1736 nm	-1909 nm	-1436 nm
Rp	1350 nm	1492 nm	1532 nm

Contact Angle Analysis

To evaluate the hydrophilicity of the fabricated adsorbents, water drop contact angle test was performed on the sample surfaces [48, 53]. Images of water drop on the surface of PLA nanofibers, and PLA nanofibers containing 5 and 10 wt% AC NPs are provided in Fig. 5. According to the obtained images,

presence and increase in the percentage of AC NPs resulted in decrease in contact angle of the water drop which means decrease in hydrophobicity of PLA nanofibers. This observation can be attributed to the increase in surface energy and changes in the morphology of PLA nanofibers at the presence of AC NPs. As can be seen, water contact angle on the surface of PLA nanofibers containing 10 wt% AC NPs is 109° and 95° at the moment and after 1 minute, respectively, which indicates the possibility of proper contact of blood with this adsorbent surface and accordingly, enhanced probability of uremic toxins binding to the adsorbent.

Partial Thromboplastin Time

In order to evaluate the tendency of the prepared adsorbent (PLA nanofibers containing 10 wt% AC NPs) to activate the coagulation cascade, partial thromboplastin time test was done. According to the result (Table 2), clot formation duration on the prepared adsorbent was 32.4 sec which is within the Thermo Fisher kit's normal range [54]. Accordingly, the prepared adsorbent, despite providing proper hydrophilic property and presence of activated carbon NPs, doesn't adversely affect the in-contact blood and doesn't accelerate the coagulation process.

Table 2
Partial Thromboplastin Time Test Results

No.	Sample	PTT (s)
1	PLA-ACN10%	32.4
2	Thermo Fisher kit's normal range	24–37

Adsorption Analysis

In order to investigate the efficiency of the fabricated adsorbents in removing uremic toxins and to determine the amount of uremic toxins removal from the containing solutions, hippuric acid and urea were considered as toxins and adsorption test was performed according to the method presented in previous section by using UV spectroscopy. In order to quantitative evaluation, calibration curves for hippuric acid and urea were prepared using solution of known concentrations from each reagent, performing UV spectroscopy on each solution, and calculating area under the peaks presented at wavelengths of 228 nm and 203 nm for hippuric acid and urea, respectively (Fig. 6d and 7d).

For the adsorption evaluation, hippuric acid solution with the initial concentration of 0.5 mg/mL was prepared and exposed to the fabricated adsorbents for 4 hours. UV spectroscopy was carried on the solutions before and after being exposure to the sorbents (Figs. 6 and 7). According to the results, hippuric acid concentration was reduced from 0.5 mg/mL in the initial solution to 0.47, 0.36, and 0.34 mg/mL after being exposed to PLA nanofibers, and PLA nanofibers containing 5 and 10 wt% AC NPs, respectively. Moreover, equilibrium adsorption capacity (qe) of hippuric acid was calculated to be 0.05, 0.1, and 0.2 for each aforementioned adsorbent. Hippuric acid removal percentage and equilibrium adsorption capacity by the fabricated adsorbents are reported in Tables 3 and 4. It is worth to be noted

that the mentioned adsorption data was achieved only with an adsorbent mass of about 3.5 mg and 0.35 mg of activated carbon NPs.

According to the results, incorporation of activated carbon nanoparticles in the PLA nanofibrous structure revealed considerable efficiency to adsorb hippuric acid, which is among the challenging protein-bonded uremic toxin. This removal capability can be related to the unique physiological properties of these NPs including the presence of nanopores which is beneficial in the adsorption of uremic toxins, especially PBUTs, together with adsorbent nanofibrous structure which provides enhance surface area [55, 56].

As the second uremic toxin, urea was considered for the evaluation of its removal by the fabricated adsorbents. For this aim, solution of this component with initial concentrations of 2.0 mg/ml was prepared and exposed to the adsorbents for 4 hours according to the procedure mentioned in the method section. Following the evaluation of the solution by UV spectrophotometer before and after being exposed to the sorbents, calculating the peak area at wavelengths of 203 nm and comparing with calibration curve, equilibrium concentration (Ce) of this toxin, removal percentage and equilibrium adsorption capacity (qe) were calculated (Tables 3 and 4). Accordingly, urea concentration was reduced from 2.0 mg/mL in the initial solution to 1.21, 0.25, and 0.19 mg/ml after being exposed to PLA nanofibers, and PLA nanofibers containing 5 and 10 wt% AC NPs, respectively. Moreover, equilibrium adsorption capacity (qe) of urea was calculated to be 1.04, 1.6 and 2.41 for each aforementioned adsorbent which demonstrates the efficacy of the prepared adsorbents in removing this toxin.

According to the results, both PLA and activated carbon played a significant role in adsorbing the urea. Only a piece of PLA nanofibrous mat with 3.5 mg weight was capable of removing about 40% of urea content. This removal capability can be related to the probable interaction with the present carboxylic groups on PLA back bone, together with adsorbent nanofibrous structure which provides enhance surface area. Furthermore, presence of 0.35 mg AC NPs in the PLA nanofibers enhanced the removal percentage to more than 90%. This outcome is achieved by both chemical composition of the fabricated sorbents and their morphology, i.e. AC NPs which brings about nanopores on the nanofibers, and nanofibrous structure which provides vast surface area, together with the existence of dual size (micro and nano) porosity.

Compared with previously reported studies, designed adsorbent in the present work provide significantly higher adsorption efficiency. For example, in one study, polylactic acid containing clay nanoparticles removed 77% of urea content[36]. In another study, polylactic acid absorbed 12% of hippuric acid, and polylactic acid containing 25% Zr-MOF (weight = 50 mg) was able to remove 57% of hippuric acid [37]. Considering the weight of applied adsorbents, much higher equilibrium adsorption capacity and consequently much higher efficiency are observed for the adsorbents designed in the present study.

Table 3
Percentage of uremic toxins removed by the prepared adsorbents.

Uremic toxin removal (%)		
Adsorbent	**HA**	Urea
PLA	**6**	39.25
PLA + 5%ACNPs	**28**	87.5
PLA + 10%ACNPs	**31**	90.5

Table 4
Equilibrium adsorption capacity (*qe*) of the prepared adsorbents.

q_e		
Adsorbent	**HA**	Urea
PLA	**0.05**	1.04
PLA + 5%ACNPs	**0.1**	1.6
PLA + 10%ACNPs	**0.2**	2.41

Morphology of the adsorbent surface after uremic toxin sorption

Figure 8 presents the SEM images of surface of the adsorbent (PLA nanofibrous mat containing 10 wt% AC NPs) after being exposed to hippuric acid solution for 4 hours. SEM images indicate the sedimentation of this compound along the nanofibers on the surface of the adsorbent, which visually proves the removal of this uremic toxin by the designed adsorbent. The intact underneath nanofibrous structure is also visible in the images.

Conclusion

In the present study, nanostructural adsorbents based on PLA nanofibers and activated carbon NPs were fabricated. Morphological evaluation revealed the average fiber diameter of 663, 445, and 699 nm, average roughness of 463, 441, and 293 nm, water contact angle of 132, 127, and 96°, hippuric acid removal percentage of 6, 28, and 31%, hippuric acid equilibrium adsorption capacity of 0.05, 0.1, and 0.2, urea removal percentage of 39.2, 87.5, and 90.5, and urea equilibrium adsorption capacity of 1, 1.6, and 2.41, for PLA nanofibrous mat, and PLA nanofibrous mat containing 5 and 10wt% AC NPs, respectively. Mentioned observations confirm that roughness of the prepared absorbents is beyond the hemolysis and RBC damage threshold. Roughness of PLA nanofibrous mat containing 10wt% AC NPs is lower than the value for the adsorption of coagulation cascade components such as platelet, fibrinogen, etc, and

this absorbent provides partial thromboplastin time of 32 seconds for the exposed human plasma which indicates no adverse clot formation.

According to the adsorption results, PLA nanofibrous structure represented good adsorptive tendency for uremic toxin removal. These observations could be related to the interaction of toxins with carboxylic acid groups and vast surface area provided by nanofibrous structure. Moreover, incorporation of just a small quantity of activated carbon NPs and their presence on the surface of PLA nanofibers significantly enhanced the uremic toxin adsorption capacity which could be attributed to the intrinsic adsorptive properties of activated carbon and innovative morphology design of the fabricated adsorbents. Adsorbent morphology comprising nanoparticles on nanofibers provides vast contact area and dual size porosity, i.e. nano porosity in AC NPs structure and micro porosity between the PLA nanofibers. Furthermore, placement of AC NPs in the nanofibers prevents their mixing with toxin solution (blood) and obviates the need for the secondary process for their gathering. According to the observations in the present study, the introduced nanostructured adsorbents have promising capabilities for being used for uremic toxins removal in hemoperfusion and in combination with hemodialysis.

Declarations

Funding:

This research received no specific funding.

Author Contribution

Authorship contribution statement:Pooya Javadi: Formal Analysis, Writing the draft.Fatemeh Hejazi: Supervision, Resources, Conceptualization, Interpretation of the results, Review & editing.Leila Malekmakan: Supervision, Interpretation of the results, Review & editing.All authors approved the version to be published.

Data Availability

All data supporting the findings of this study are available within the paper. Raw data are available upon request from the corresponding author.

References

1. Khajehdehi P et al (2014) *Prevalence of chronic kidney disease and its contributing risk factors in southern Iran a cross-sectional adult population-based study.*
2. Qin K et al (2024) Epidemiological shifts in chronic kidney disease: a 30-year global and regional assessment. BMC Public Health 24(1):3519

3. Chen J et al (2025) Global, regional, and national trends in chronic kidney disease burden (1990–2021): a systematic analysis of the global burden of disease in 2021. Trop Med Health 53(1):1–17
4. Nubé MJ, Grooteman MP, Blankestijn PJ (2015) Hemodiafiltration: theory, technology and clinical practice. Springer
5. Xu Y et al (2023) Derivation and elimination of uremic toxins from kidney-gut axis. Front Physiol 14:1123182
6. Magnani S, Atti M (2021) Uremic toxins and blood purification: a review of current evidence and future perspectives. Toxins 13(4):246
7. Maheshwari V et al (2019) In silico comparison of protein-bound uremic toxin removal by hemodialysis, hemodiafiltration, membrane adsorption, and binding competition. Sci Rep 9(1):909
8. Cheng Y-C et al (2018) Clearance of low molecular-weight uremic toxins p-cresol, creatinine, and urea from simulated serum by adsorption. J Mol Liq 252:203–210
9. Han SS et al (2015) Dialysis modality and mortality in the elderly: a meta-analysis. Clin J Am Soc Nephrol 10(6):983–993
10. Abdelhameed RM et al (2025) Efficient uremic toxins adsorption from simulated blood by immobilization of metal organic frameworks anchored Sephadex beads. Sci Rep 15(1):9667
11. Huang Y et al (2024) A review: current urea sorbents for the development of a wearable artificial kidney. J Mater Sci 59(26):11669–11686
12. Ma Y et al (2021) Adsorption-based strategies for removing uremic toxins from blood. Microporous Mesoporous Mater 319:111035
13. Cheah WK et al (2017) Nanoporous biomaterials for uremic toxin adsorption in artificial kidney systems: A review. J Biomedical Mater Res Part B: Appl Biomaterials 105(5):1232–1240
14. Yatzidis H (1972) Activated charcoal rediscovered. BMJ 4(5831):51
15. Chirito E et al (1977) Artificial liver: the effect of ACAC microencapsulated charcoal hemoperfusion on fulminant hepatic failure. Artif Organs 1(1):76–83
16. Yarmush ML, Dunn JC, Tompkins RG (1992) Assessment of artificial liver support technology. Cell Transplant 1(5):323–341
17. Yoshiba M et al (1996) Favorable effect of new artificial liver support on survival of patients with fulminant hepatic failure. Artif Organs 20(11):1169–1172
18. Singh KP et al (2003) Color removal from wastewater using low-cost activated carbon derived from agricultural waste material. Ind Eng Chem Res 42(9):1965–1976
19. Tan I, Ahmad AL, Hameed B (2008) Adsorption of basic dye on high-surface-area activated carbon prepared from coconut husk: Equilibrium, kinetic and thermodynamic studies. J Hazard Mater 154(1–3):337–346
20. Wang J et al (2008) The porous structures of activated carbon aerogels and their effects on electrochemical performance. J Power Sources 185(1):589–594

21. Sandeman SR et al (2014) An adsorbent monolith device to augment the removal of uraemic toxins during haemodialysis. J Mater Science: Mater Med 25(6):1589–1597
22. Pavlenko D et al (2017) Carbon adsorbents with dual porosity for efficient removal of uremic toxins and cytokines from human plasma. Sci Rep 7(1):14914
23. Grylewicz A, Mozia S (2021) Polymeric mixed-matrix membranes modified with halloysite nanotubes for water and wastewater treatment: A review. Sep Purif Technol 256:117827
24. Dharupaneedi SP et al (2019) Membrane-based separation of potential emerging pollutants. Sep Purif Technol 210:850–866
25. Galiano F et al (2018) Advances in biopolymer-based membrane preparation and applications. J Membr Sci 564:562–586
26. Zhao J et al (2011) Improved biocompatibility and antifouling property of polypropylene non-woven fabric membrane by surface grafting zwitterionic polymer. J Membr Sci 369(1–2):5–12
27. Jo G, Kwon J, Kang HS (2024) Engineering electrospun PAN/PCL blend for high-performance and eco-friendly particulate matter filtration. Reactive Funct Polym 204:106026
28. Kishor R, Bharagava RN, Saxena G (2018) *Industrial wastewaters: the major sources of dye contamination in the environment, ecotoxicological effects, and bioremediation approaches*, in *Recent advances in environmental management*. CRC, pp 1–25
29. Rasal RM, Janorkar AV, Hirt DE (2010) Poly (lactic acid) modifications. Prog Polym Sci 35(3):338–356
30. Bettahalli N et al (2011) Development of poly (l-lactic acid) hollow fiber membranes for artificial vasculature in tissue engineering scaffolds. J Membr Sci 371(1–2):117–126
31. Ellis MJ, Chaudhuri JB (2007) Poly (lactic-co-glycolic acid) hollow fibre membranes for use as a tissue engineering scaffold. Biotechnol Bioeng 96(1):177–187
32. Ma Z et al (2005) Cartilage tissue engineering PLLA scaffold with surface immobilized collagen and basic fibroblast growth factor. Biomaterials 26(11):1253–1259
33. Shi S et al (2010) Preparation and characterization of microporous poly (D, L-lactic acid) film for tissue engineering scaffold. Int J Nanomed, : p. 1049–1055
34. Hu W, Huang ZM (2010) Biocompatibility of braided poly (L-lactic acid) nanofiber wires applied as tissue sutures. Polym Int 59(1):92–99
35. Bergsma JE et al (1995) Late degradation tissue response to poly (L-lactide) bone plates and screws. Biomaterials 16(1):25–31
36. Andrade-Guel M et al (2021) Nanocomposite PLA/C20A nanoclay by ultrasound-assisted melt extrusion for adsorption of uremic toxins and methylene blue dye. Nanomaterials 11(10):2477
37. Zeng S et al (2022) Adsorptive removal of uremic toxins using Zr-based MOFs for potential hemodialysis membranes. J Mater Sci 57(4):2909–2923
38. Xiong S (2022) *Development of Absorbents Based on Polymeric Nanocomposites for Uraemic Toxin Sorption*. UCL (University College London)

39. Casasola R et al (2014) Electrospun poly lactic acid (PLA) fibres: Effect of different solvent systems on fibre morphology and diameter. Polymer 55(18):4728–4737
40. Hejazi F (2024) Innovative Nanofibrous Dini's Surface as a Three-Dimensional Highly Porous Scaffold Providing Enhanced Cellular Infiltration. Polym Adv Technol 35(12):e70023
41. Hejazi F et al (2017) Novel class of collector in electrospinning device for the fabrication of 3D nanofibrous structure for large defect load-bearing tissue engineering application. J Biomedical Mater Res Part A 105(5):1535–1548
42. Hejazi F, Mirzadeh H, Shojaei S (2023) PCL-based 3D nanofibrous structure with well-designed morphology and enhanced specific surface area for tissue engineering application. Prog Biomater 12(2):113–122
43. Hejazi F et al (2021) Fabrication of nanocomposite/nanofibrous functionally graded biomimetic scaffolds for osteochondral tissue regeneration. J biomedical Mater Res part A 109(9):1657–1669
44. Hejazi F et al (2021) Improved healing of critical-size femoral defect in osteoporosis rat models using 3D elastin/polycaprolactone/nHA scaffold in combination with mesenchymal stem cells. J Mater Science: Mater Med 32(3):27
45. Hejazi F, Mirzadeh H (2016) Novel 3D scaffold with enhanced physical and cell response properties for bone tissue regeneration, fabricated by patterned electrospinning/electrospraying. J Mater Science: Mater Med 27(9):143
46. Hejazi F, Zare F, Asgari M (2024) Enhanced differentiation of mesenchymal stem cells in coral-incorporated PCL/elastin scaffold enables 3D defect healing in osteoporosis rat model. Int J Biol Macromol 277:134483
47. Mirbehbahani FS et al (2020) Artemisia annua L. as a promising medicinal plant for powerful wound healing applications. Prog Biomater 9(3):139–151
48. Law K-Y (2014) Definitions for hydrophilicity, hydrophobicity, and superhydrophobicity: getting the basics right. ACS Publications. p. 686–688
49. Xia F, Rangelow IW, Youcef-Toumi K (2024) Active Probe Atomic Force Microscopy. Springer Nature
50. Maruyama O et al (2006) HEMOLYTIC STUDY RELATED TO BLOOD-CONTACTING AREA WITH SURFACE ROUGHNESS UNDER SHEAR FLOW CONDITIONS: S3–4. Artif Organs 30(11):A31–A32
51. Maruyama O et al (2006) Hemolysis resulting from surface roughness under shear flow conditions using a rotational shear stressor. Artif Organs 30(5):365–370
52. Linneweber J et al (2007) The effect of surface roughness on activation of the coagulation system and platelet adhesion in rotary blood pumps. Artif Organs 31(5):345–351
53. Liu K, Sorgato M, Savio E (2025) From Hydrophilic to Superhydrophobic: Tuning Surface Wettability through Salvinia-Inspired Topographies. ACS Appl Mater Interfaces 17(31):45066–45081
54. Adcock D et al (2024) International Council for Standardization in Haematology (ICSH) recommendations for the performance and interpretation of activated partial thromboplastin time and prothrombin time mixing tests. Int J Lab Hematol 46(5):777–788

55. Rodrigues FS, Faria M (2023) Adsorption-and displacement-based approaches for the removal of protein-bound uremic toxins. Toxins 15(2):110
56. Yang C et al (2024) Mesoporous activated carbon derived from Chinese herbal medicine residues for hemoperfusion removal of uremia toxins from progressive chronic kidney diseases patients. Heliyon, 10(20)

Figures

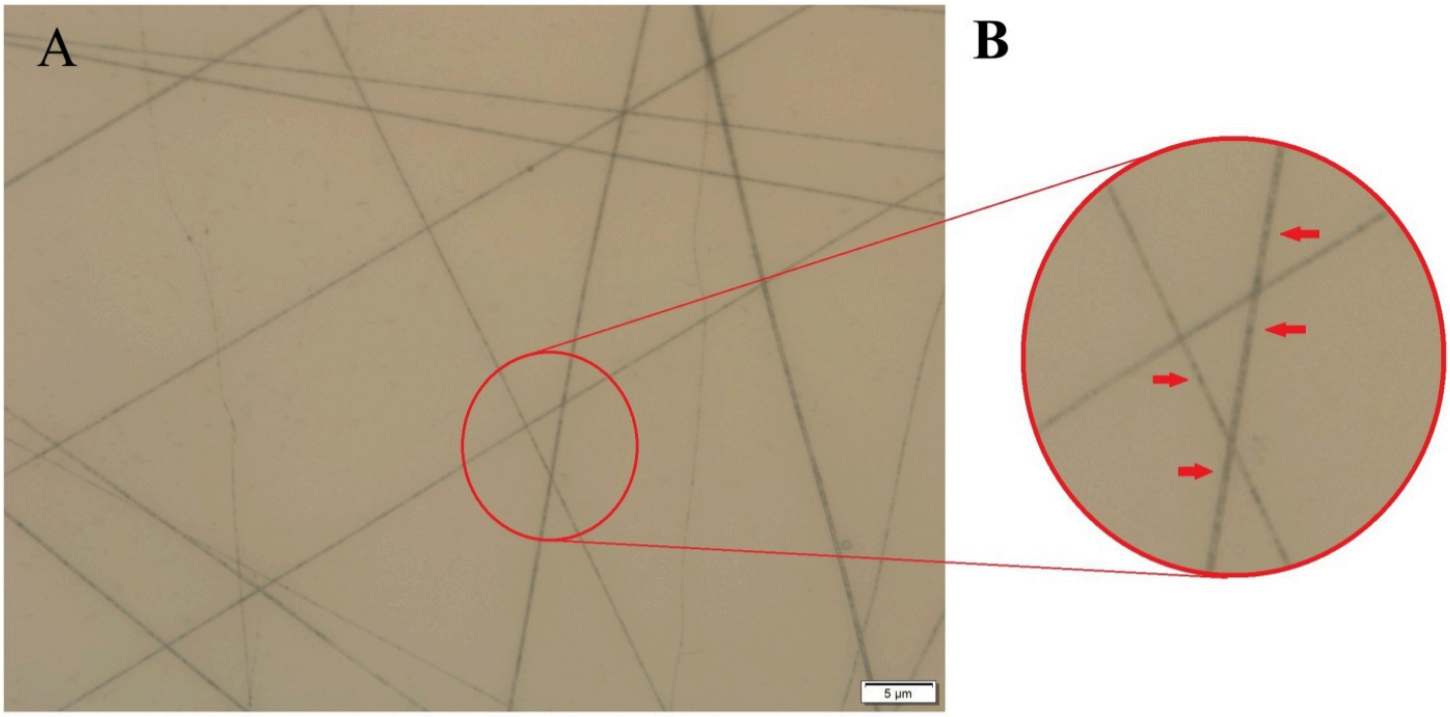


Figure 1

Optical microscope images of A) PLA nanofibers containing 5% activated carbon NPs at 40x magnification, B) Magnified portion of the image with obvious NPs within the nanofibers marked by red flashes.

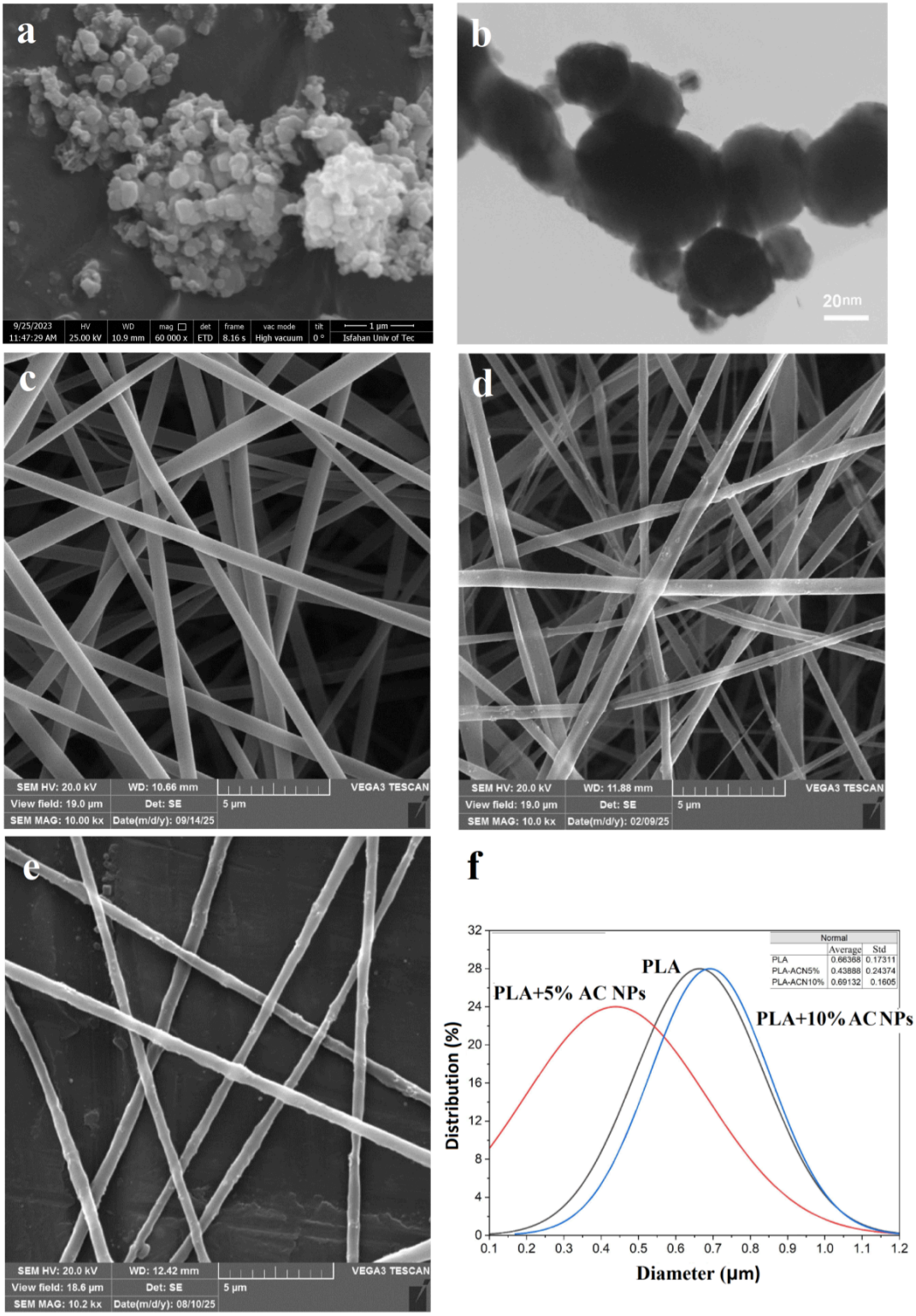


Figure 2

a and b) SEM and TEM images of the AC NPs (provided by the manufacturer, Iranian Nanomaterials Pioneers Company, Iran). c, d, e) SEM images of the adsorbent surface, i.e. PLA nanofibers, PLA nanofibers containing 5 wt% AC NPs, and PLA nanofibers containing 10wt% AC NPs, respectively. f) Nanofibers diameter distribution curves of the adsorbents.

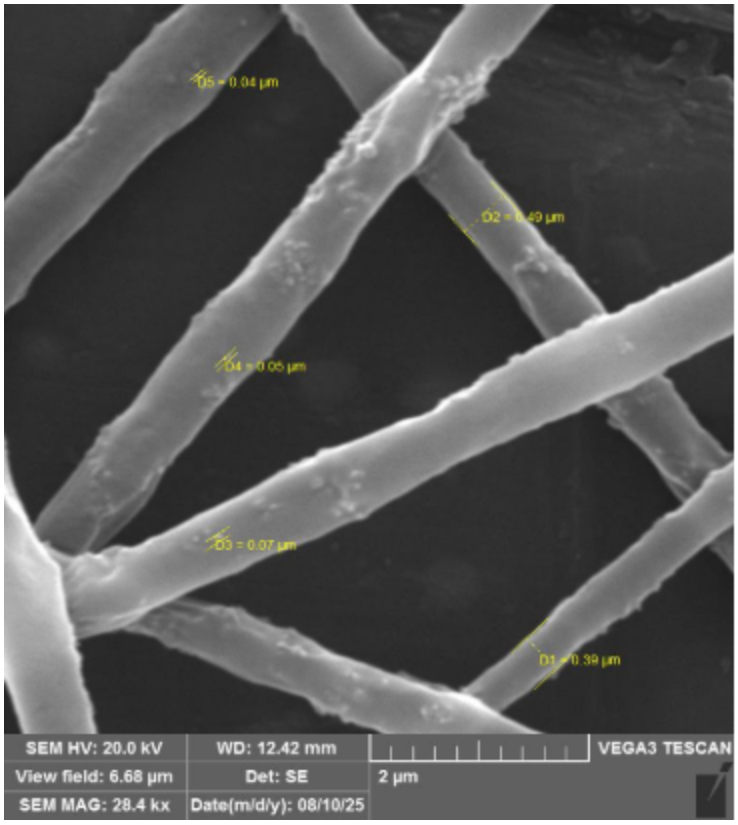


Figure 3

SEM image of PLA nanofibers containing 10 wt% AC NPs (at 28k magnification), representing AC NPs on the surface of nanofibers.

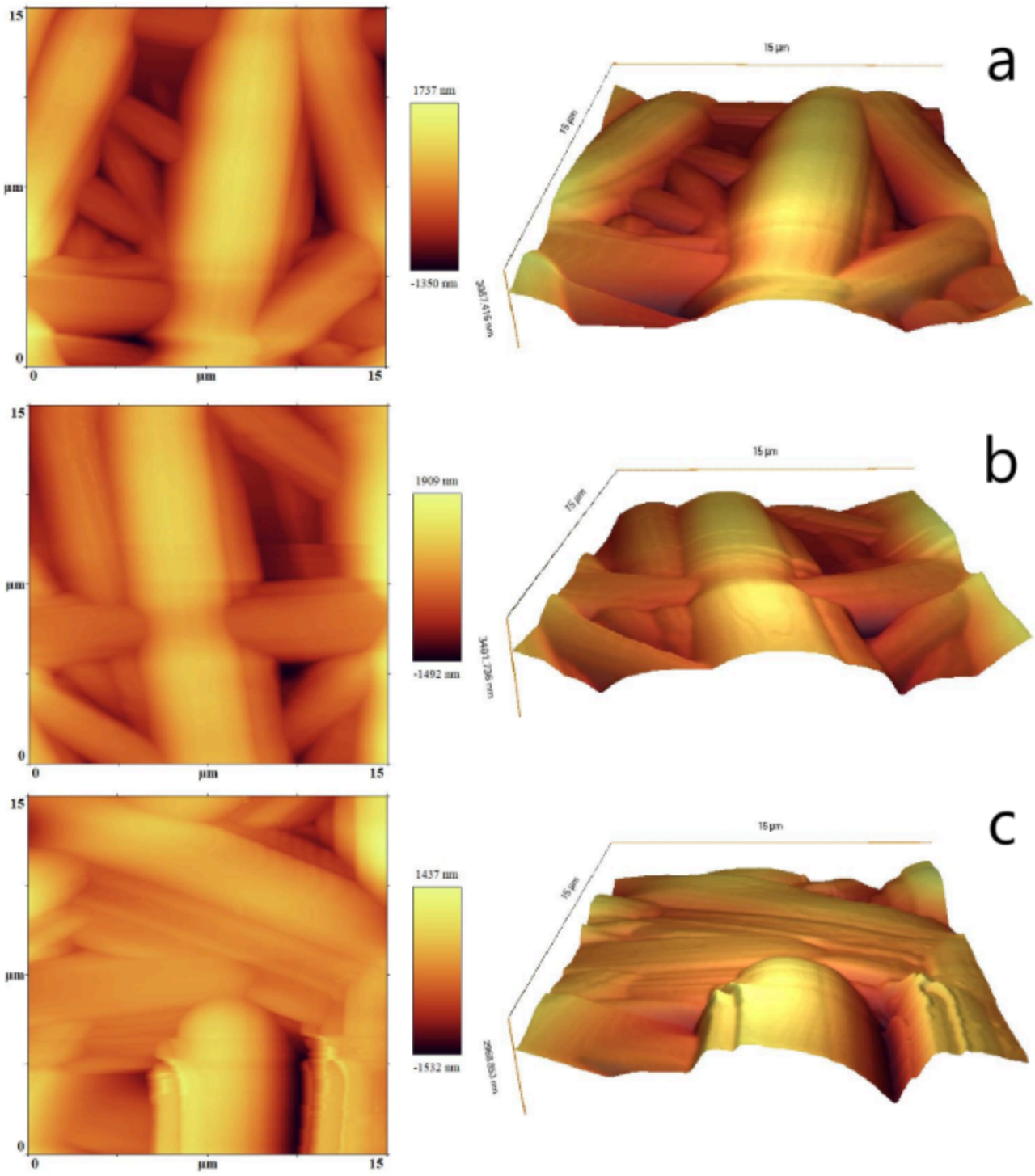


Figure 4

AFM images of the adsorbent surface a) PLA nanofibrous mat, b) PLA nanofibrous mat containing 5 wt% AC NPs, and c) PLA nanofibrous mat containing 10 wt% AC NPs.

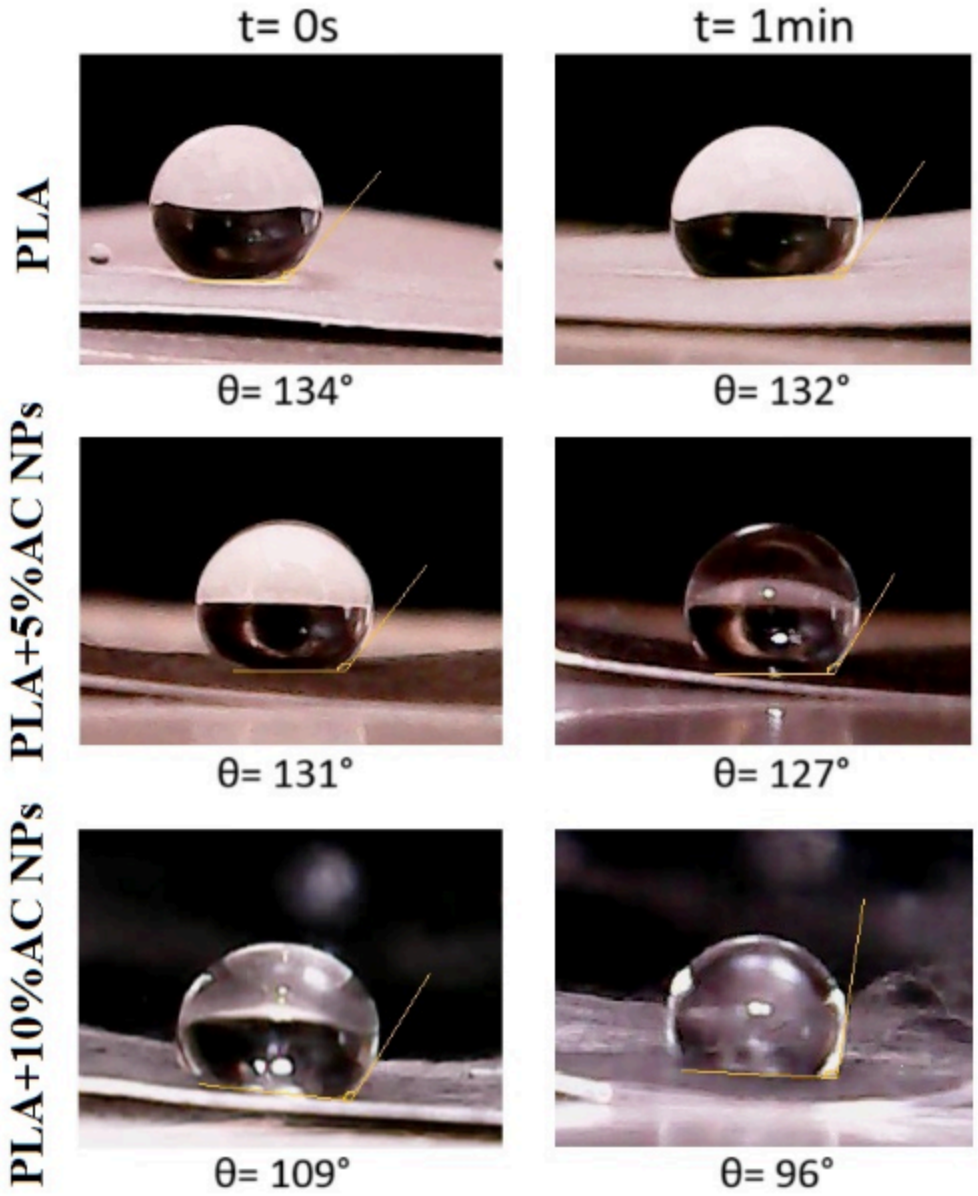


Figure 5

Water contact angle on the prepared absorbents.

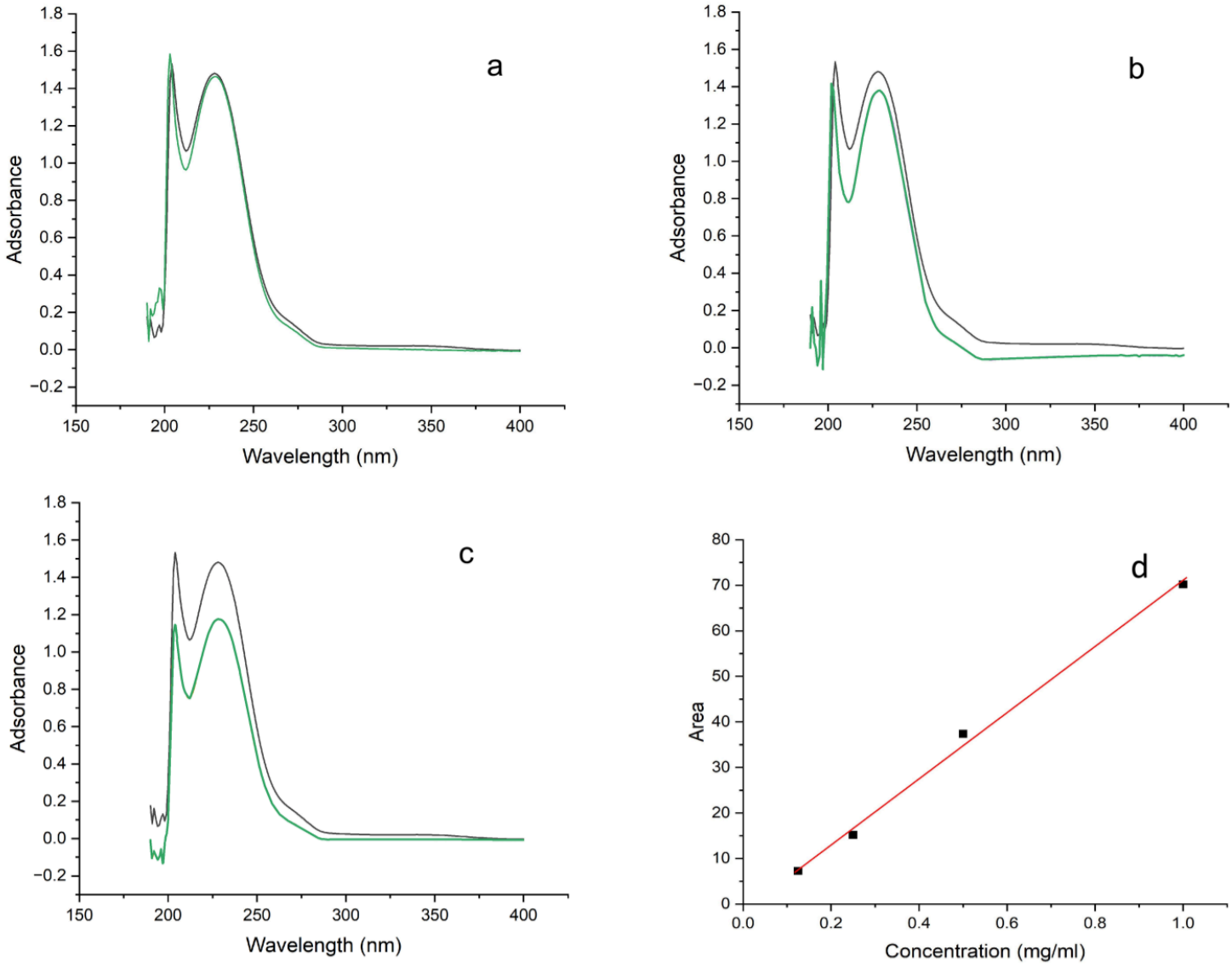


Figure 6

Ultraviolet spectra of initial hippuric acid solution (black line) and hippuric acid solution after being exposed (green lines) to: a) PLA nanofibrous mat, b) PLA nanofibrous mat containing 5 wt% AC NPs, and c) PLA nanofibrous mat containing 10 wt% AC NPs. d) hippuric acid solution calibration curve.

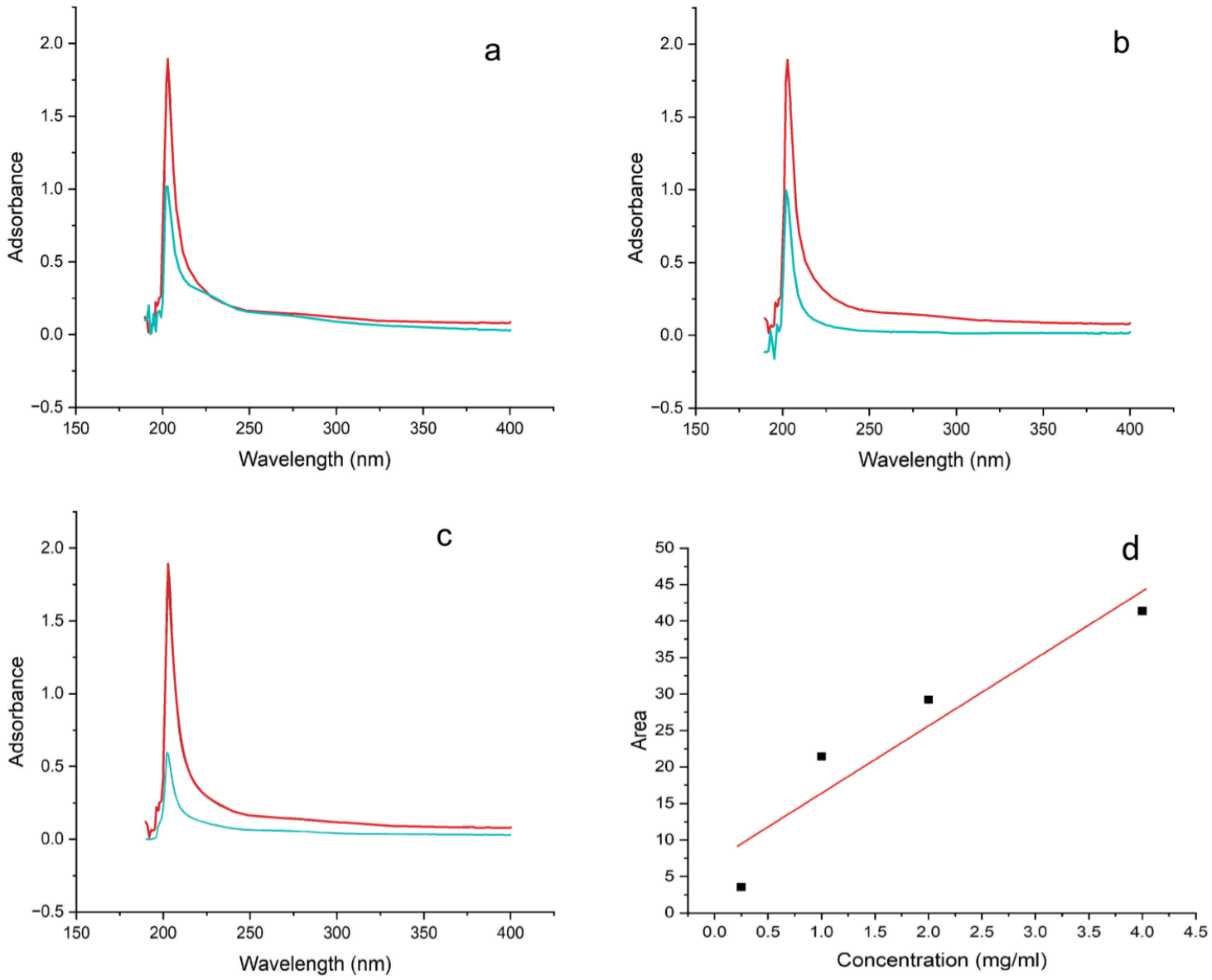


Figure 7

Ultraviolet spectra of initial urea solution (red line) and urea solution after being exposed (blue lines) to: a) PLA nanofibrous mat, b) PLA nanofibrous mat containing 5 wt% AC NPs, and c) PLA nanofibrous mat containing 10 wt% AC NPs. d) Urea solution calibration curve.

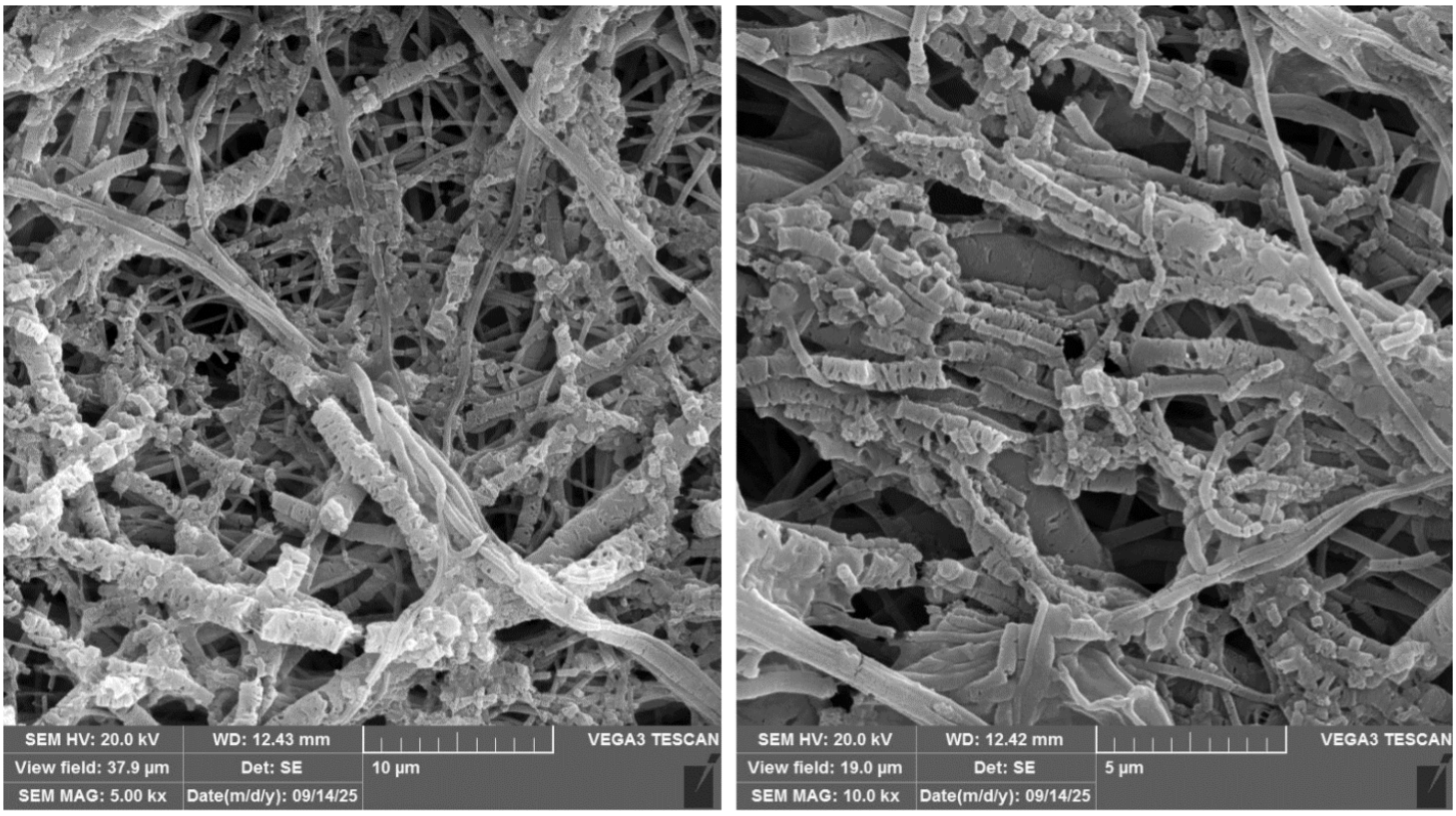


Figure 8

SEM images of the surface of PLA nanofibrous mat containing 10 wt% AC NPs after being exposed to hippuric acid, at 5,000 and 10,000x magnifications.